

Meissner screening mass in two-flavor quark matter at nonzero temperature

O. Kiriyama*

Institut für Theoretische Physik, J.W. Goethe-Universität, D-60438 Frankfurt am Main, Germany

(Dated: April 28, 2018)

We calculate the Meissner screening mass of gluons 4–7 in two-flavor quark matter at nonzero temperature. To this end, we study the effective potential of the 2SC/g2SC phases including a vector condensate $\langle gA_z^6 \rangle$ and calculate the Meissner mass from the potential curvature with respect to $\langle gA_z^6 \rangle$. We find that the Meissner mass becomes real at the critical temperature which is about the half of the chemical potential mismatch. The phase diagram of the neutral two-flavor color superconductor is presented in the plane of temperature and coupling strength. We indicate the unstable region for gluons 4–7 on the phase diagram.

PACS numbers: 12.38.-t, 11.30.Qc, 26.60.+c

During the last decade, significant advances have been made in our understandings of color superconductivity. The studies of QCD-motivated effective theories have revealed a rich phase structure of neutral quark matter [1]. However, the question which phase is realized in nature is still inconclusive because of a chromomagnetic instability [2, 3, 4, 5]. (For recent discussions on this issue, see also Refs. [6, 7, 8, 9, 10, 11, 12, 13, 14, 15, 16].)

In the two-flavor case (and at zero temperature), while the 8th gluon has a tachyonic Meissner mass in the region $\Delta/\delta\mu < 1$ (Δ is a diquark gap and $\delta\mu$ denotes the chemical potential mismatch between up and down quarks), the more severe instability related to gluons 4–7 emerges in the region $\Delta/\delta\mu < \sqrt{2}$ (i.e. not only in the g2SC phase but also in the 2SC phase) [2].

At nonzero temperature, the instability is expected to be weakened by thermal effects [4, 5]. In this work, we calculate the Meissner screening mass of gluons 4–7 in two-flavor quark matter at nonzero temperature that has not been addressed so far. The results are useful for the phase diagram of QCD and compact star phenomenology.

To study the Meissner screening mass of gluons 4–7, we use a gauged Nambu–Jona-Lasinio (NJL) model with massless up and down quarks:

$$\mathcal{L} = \bar{\psi}(i\cancel{D} + \hat{\mu}\gamma^0)\psi + G_D (\bar{\psi}i\gamma_5\epsilon^b C\bar{\psi}^T)(\psi^T C i\gamma_5\epsilon^b \psi) - \frac{1}{4}F_{\mu\nu}^a F^{a\mu\nu}, \quad (1)$$

where the quark field ψ carries flavor ($i, j = 1, \dots, N_f$ with $N_f = 2$) and color ($\alpha, \beta = 1, \dots, N_c$ with $N_c = 3$) indices, C is the charge conjugation matrix; $(\epsilon)^{ik} = \epsilon^{ik}$ and $(\epsilon^b)^{\alpha\beta} = \epsilon^{b\alpha\beta}$ are the antisymmetric tensors in flavor and color spaces, respectively. The covariant derivative and the field-strength tensor are defined as

$$D_\mu = \partial_\mu - igA_\mu^a T^a, \quad (2a)$$

$$F_{\mu\nu}^a = \partial_\mu A_\nu^a - \partial_\nu A_\mu^a + g f^{abc} A_\mu^b A_\nu^c. \quad (2b)$$

In order to evaluate loop diagrams we use a three-momentum cutoff $\Lambda = 653.3$ MeV. This specific choice does not affect the qualitative features of the present analysis.

In NJL-type models, one has to impose the neutrality conditions by adjusting the values of an electron chemical potential μ_e and a color chemical potential μ_8 [17]. We neglect the color chemical potential μ_8 throughout because it is suppressed in the 2SC/g2SC phases, $\mu_8 \ll \Delta$. Then, the elements of the diagonal matrix of quark chemical potentials $\hat{\mu}$ in β -equilibrated neutral quark matter are given by $\mu_u = \bar{\mu} - \delta\mu$ and $\mu_d = \bar{\mu} + \delta\mu$ with $\bar{\mu} = \mu - \delta\mu/3$ and $\delta\mu = \mu_e/2$.

In Nambu–Gor’kov space, the inverse full quark propagator $S^{-1}(p)$ is written as

$$S^{-1}(p) = \begin{pmatrix} (S_0^+)^{-1} & \Phi^- \\ \Phi^+ & (S_0^-)^{-1} \end{pmatrix}, \quad (3)$$

with

$$(S_0^+)^{-1} = \gamma^\mu p_\mu + (\bar{\mu} - \delta\mu\tau^3)\gamma^0 + g\gamma^\mu A_\mu^a T^a, \quad (4a)$$

$$(S_0^-)^{-1} = \gamma^\mu p_\mu - (\bar{\mu} - \delta\mu\tau^3)\gamma^0 - g\gamma^\mu A_\mu^a T^{aT}, \quad (4b)$$

and

$$\Phi^- = -i\epsilon^b\gamma_5\Delta, \quad \Phi^+ = -i\epsilon^b\gamma_5\Delta. \quad (5)$$

Here $\tau^3 = \text{diag}(1, -1)$ is a matrix in flavor space. We have chosen the diquark condensate to point in the third direction in color space. In this work we are interested in the Meissner screening mass of gluons 4–7, so it is sufficient to study the case of the nonvanishing vector condensate $B \equiv \langle gA_z^6 \rangle \neq 0$ [9].

In the one-loop approximation, the effective potential of two-flavor quark matter with electrons at finite temperature T is given by

$$\begin{aligned} V(\Delta, B, \delta\mu, \mu, T) = & -\frac{1}{12\pi^2} \left(\mu_e^4 + 2\pi^2 T^2 \mu_e^2 + \frac{7\pi^4}{15} T^4 \right) \\ & + \frac{\Delta^2}{4G_D} - \frac{T}{2} \sum_{n=-\infty}^{\infty} \int_{-\Lambda}^{\Lambda} \frac{d^3 p}{(2\pi)^3} \\ & \times \ln \text{Det} S^{-1}(i\omega_n, \vec{p}), \end{aligned} \quad (6)$$

*Electronic address: kiriyama@th.physik.uni-frankfurt.de

where $\omega_n = (2n + 1)\pi T$ are the Matsubara frequencies ($n = 0, \pm 1, \pm 2, \dots$).

Let us look at the Meissner screening mass derived from the effective potential (6). Although the potential curvature reproduce the correct hard-dense-loop (HDL) result for the Meissner mass squared at zero temperature [9, 15],

$$\begin{aligned} \frac{\partial^2 V(\Delta, B, \delta\mu, \mu, 0)}{\partial B^2} \Big|_{B=0} \\ = \frac{\bar{\mu}^2}{6\pi^2} \left[1 - \frac{2\delta\mu^2}{\Delta^2} + 2 \frac{\delta\mu\sqrt{\delta\mu^2 - \Delta^2}}{\Delta^2} \theta(\delta\mu - \Delta) \right], \end{aligned} \quad (7)$$

this is not the case for the Meissner mass squared calculated directly from Eq. (6). [Note that terms of order $\mathcal{O}(\bar{\mu}^2/\Lambda^2)$ and $\mathcal{O}(\Delta^2/\bar{\mu}^2)$ have been neglected in Eq. (7).] The potential curvature suffers from ultraviolet divergences $\propto \Lambda^2$ and therefore we have to subtract them.

At zero temperature the subtraction term is given by

$$\frac{\partial^2 V(0, B, 0, 0, 0)}{\partial B^2} \Big|_{B=0} = -\frac{\Lambda^2}{3\pi^2}. \quad (8)$$

At nonzero temperature, since we use a finite cutoff, the subtraction term should depend on temperature. Indeed one finds

$$\begin{aligned} \frac{\partial^2 V(0, B, \delta\mu, \mu, T)}{\partial B^2} \Big|_{B=0} \\ = \frac{\Lambda^2}{12\pi^2} \sum_{e1, e2, e3=\pm} e_1 N_F(e_1 \Lambda + e_2 \bar{\mu} + e_3 \delta\mu), \end{aligned} \quad (9)$$

where $N_F(x) = 1/(e^{x/T} + 1)$, otherwise the Meissner mass in the normal phase assumes an unphysical positive value. Note that, in the case of $T \rightarrow 0$, Eq. (9) is in exact agreement with Eq. (8). It should be also noted that the temperature dependence in Eq. (9) is made redundant when $\Lambda \gg T$. Thus, the temperature dependence of Eq. (9) is a cutoff artifact indeed.

Figure 1 shows the Meissner mass squared,

$$\begin{aligned} m_M^2 = \frac{\partial^2}{\partial B^2} [V(\Delta, B, \delta\mu, \mu, T) \\ - V(0, B, \delta\mu, \mu, T)] \Big|_{B=0}, \end{aligned} \quad (10)$$

as a function of $\Delta/\delta\mu$ for several temperatures. The results are plotted for $\bar{\mu} = 500$ MeV and $\delta\mu = 80$ MeV. Note that we have solved neither the gap equation nor the neutrality condition, thus $\Delta/\delta\mu$ in Fig. 1 are temperature independent parameters.

At $T = 0$, we see the manifestation of the chromomagnetic instability at all values below $\Delta/\delta\mu = \sqrt{2}$. (Since our model parameters do not correspond to the HDL limit, strictly speaking, the actual critical value of $\Delta/\delta\mu$ is somewhat smaller than $\sqrt{2}$.) As T is increased, due to thermal smoothing effects, the Meissner mass squared

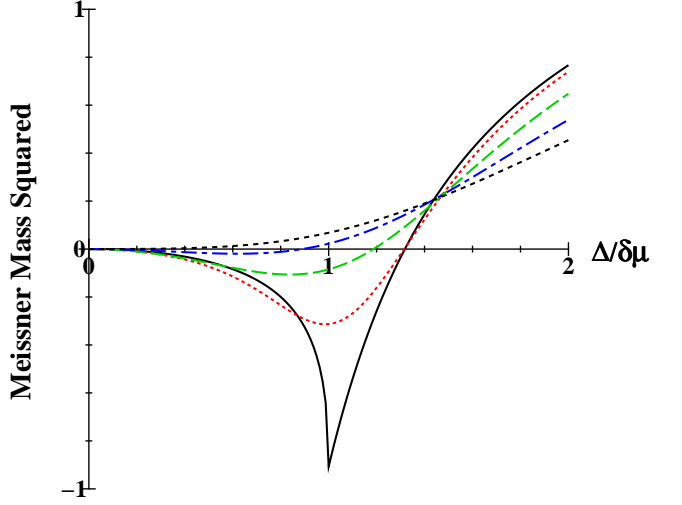


FIG. 1: The Meissner mass squared [divided by $\bar{\mu}^2/(6\pi^2)$] as a function of $\Delta/\delta\mu$ for $T = 0$ MeV (solid), $T = 10$ MeV (dotted), $T = 20$ MeV (dashed), $T = 30$ MeV (dot-dashed), $T = 40$ MeV (short-dashed). We used $\bar{\mu} = 500$ MeV and $\delta\mu = 80$ MeV.

tends to approach its value in the normal phase. However, its temperature dependence at fixed $\Delta/\delta\mu$ shows a non-monotonic behavior. This is analogous to the result for a charged condensate reported in Ref. [4].

The Meissner mass squared at small but nonzero values of $\Delta/\delta\mu$ remains negative at higher temperatures. At $T^* \simeq \delta\mu/2 \simeq 40$ MeV, the imaginary Meissner mass completely disappears for all values of $\Delta/\delta\mu$ [24]. As T is further increased, the Meissner mass squared at nonzero values of $\Delta/\delta\mu$ begins to become small and approaches zero. (Note that, due to the normalization (10), m_M^2 in the normal phase, $\Delta/\delta\mu = 0$, is always zero.)

In order to investigate the implications of our analysis for the phase structures of QCD, we solved the gap equation and the neutrality condition:

$$\frac{\partial V(\Delta, 0, \delta\mu, \mu, T)}{\partial \Delta} = 0, \quad (11a)$$

$$\frac{\partial V(\Delta, 0, \delta\mu, \mu, T)}{\partial \mu_e} = 0. \quad (11b)$$

The phase diagram of the neutral 2SC/g2SC matter is displayed in Fig. 2 as a function of T and Δ_0 . Here, Δ_0 is the value of the 2SC gap at $\delta\mu = 0$ and at $T = 0$. The result is plotted for $\mu = 400$ MeV, which should be relevant to the interior of compact stars. The solid (dashed) line denotes the critical line of the phase transition between the normal quark phase and the g2SC phase (the g2SC phase and the 2SC phase). At $T = 0$, the g2SC phase exists in the window

$$92 \text{ MeV} < \Delta_0 < 134 \text{ MeV}, \quad (12)$$

and the 2SC window is given by

$$\Delta_0 > 134 \text{ MeV}. \quad (13)$$

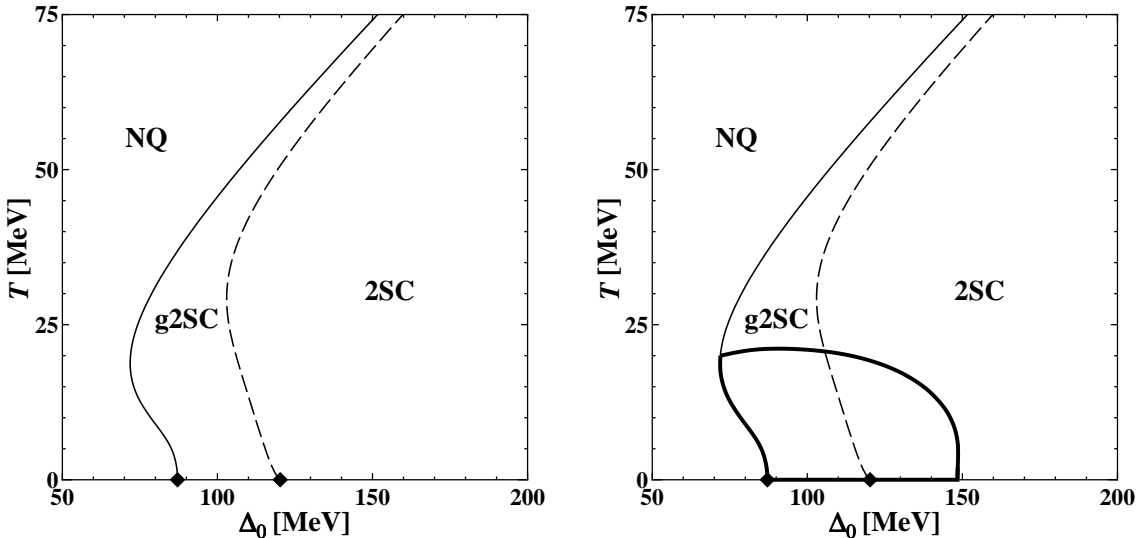


FIG. 2: Left: The phase diagram of neutral two-flavor color superconductor as a function of T and Δ_0 . The solid (dashed) line denotes the critical line of the phase transition between the normal quark phase and the g2SC phase (the g2SC phase and the 2SC phase). The results are plotted for $\mu = 400$ MeV. Right: The same as the left panel, but the unstable region for gluons 4–7 is enclosed by the thick solid line.

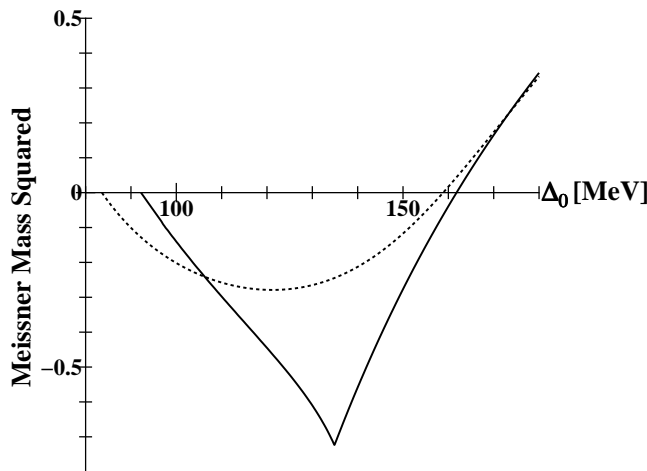


FIG. 3: The Meissner mass squared [divided by $\bar{\mu}^2/(6\pi^2)$] as a function of Δ_0 for $T = 0$ MeV (solid) and $T = 10$ MeV (dotted). The results are plotted for $\mu = 400$ MeV. At $T = 0$ MeV, the curve has a kink at the onset of the g2SC phase.

These results agree with those obtained by using an approximation for the effective potential [10, 15]. As we will see below, the phase diagram in the left panel of Fig. 2 is qualitatively consistent with those presented in the literature [18, 19].

In the weak coupling regime, $77 \text{ MeV} < \Delta_0 < 92 \text{ MeV}$, the chemical potential mismatch is too large for these couplings for diquark pairing and the system is in the normal quark (NQ) phase at $T = 0$. At $T > 0$, the mismatch of the Fermi surfaces is thermally smeared and, then, it opens the possibility of finding the g2SC phase. In the intermediate coupling regime, $92 \text{ MeV} < \Delta_0 < 134 \text{ MeV}$,

we find the g2SC phase even at $T = 0$. For relatively strong couplings, $110 \text{ MeV} < \Delta_0 < 134 \text{ MeV}$, the g2SC phase at low temperature is replaced by the 2SC phase at intermediate temperature. At higher temperature, the 2SC phase is replaced by the g2SC phase again. It is known that this unusual behavior happens in the intermediately coupled two-flavor color superconductor [18]. For strong coupling, $\Delta_0 > 134 \text{ MeV}$, the gap Δ increases and the 2SC phase is favored at $T = 0$. At higher temperatures, however, Δ is decreased by thermal effects and the g2SC phase becomes possible.

Let us now take into account the chromomagnetic instability. Combining Eq. (11) with the Meissner mass squared (10), we calculated the Meissner mass squared and mapped out the unstable region for gluons 4–7 on the T - Δ_0 phase diagram. The region enclosed by the solid thick line in the right panel of Fig. 2 corresponds to the region where gluons 4–7 have a negative Meissner mass squared. In this region, the gluonic phase is energetically more favored than the 2SC/g2SC phases and resolves the instability. (In this paper, we refer to the phase where $B \neq 0$ as the gluonic phase. Strictly speaking, the reduced symmetry of the 2SC/g2SC phases with $B \neq 0$ does not exclude additional gluonic condensates [9].)

At $T = 0$, we find the manifestation of the instability in the region $92 \text{ MeV} < \Delta_0 < 162 \text{ MeV}$ (see Fig. 3) [25]. For extremely strong couplings, $\Delta_0 \gtrsim 162 \text{ MeV}$, the 2SC phase is free from the instability not only at $T = 0$ but also at $T > 0$. On the other hand, the whole g2SC phase and the part of the 2SC phase suffer from the instability at low temperatures. At $T \simeq 20$ MeV, the phase transition from the gluonic phase to the 2SC/g2SC phases occurs and the unstable region disappears. (The order of

the phase transition is most probably second-order [20].) As is clear from the right panel of Fig. 2, in the g2SC window, the critical temperature for the gluonic \rightarrow g2SC reaches about half that for the g2SC \rightarrow NQ transition. As a consequence, most of the g2SC phase should be replaced by the gluonic phase. In addition, it is very likely that the g2SC phase is also unstable for the 8th gluon at $T \geq 0$ [4]. (Our preliminary study shows that, for intermediate couplings, the unstable region for the 8th gluon survives for temperatures of order of 10 MeV [20].) Thus, the g2SC phase suffers from the severe instability related to gluons 4–7 and 8. It should be emphasized, however, that the stable g2SC phase is not excluded from the phase diagram. Even if we take account of the instability for the 8th gluon, we still find the stable g2SC phase in high-temperature regions of the phase diagram [20], though the gapless structure is not so important at nonzero temperature.

In this paper, we studied the Meissner mass squared in the 2SC/g2SC phases at nonzero temperature. It was found that the negative Meissner mass squared for gluons 4–7 completely disappears at the temperature $T^* \simeq \delta\mu/2$. We also investigated the T - Δ_0 phase diagram and mapped out the unstable region for gluons 4–7 on the phase diagram. We did not vary the quark chemi-

cal potential μ , so we could not map out unstable regions explicitly on the T - μ phase diagram. However, the result is an indication that wide regions of the g2SC phase on the phase diagram suffer from the instability.

Resolving the chromomagnetic instability is the most pressing task in the study of the phase diagram of color super conductor. It is, therefore, interesting to reconsider the T - μ phase diagram of QCD, taking into account a LOFF state with realistic crystal structures [21, 22], a colored crystalline phase [5], a phase with a vector condensate [7, 8] and gluonic condensates [9]. Such a study would have important implications for the physics of compact stars

Acknowledgments

The author would like to thank Igor Shovkovy for fruitful discussions and Dirk Rischke for comments on the manuscript. This work was supported by the Deutsche Forschungsgemeinschaft (DFG).

Note added. After finishing this work, I learned that an overlapping study was recently done by L. He, M. Jin, and P. Zhuang [23].

[1] K. Rajagopal and F. Wilczek, in *At the Frontier of Particle Physics/Handbook of QCD*, edited by M. Shifman (World Scientific, Singapole, 2001); M. G. Alford, *Ann. Rev. Nucl. Part. Sci.* **51**, 131 (2001); D. K. Hong, *Acta. Phys. Pol. B* **32**, 1253 (2001); S. Reddy, *Acta. Phys. Pol. B* **33**, 4101 (2002); D. H. Rischke, *Prog. Part. Nucl. Phys.* **52**, 197 (2004); M. Buballa, *Phys. Rept.* **407**, 205 (2005); M. Huang, *Int. J. Mod. Phys. E* **14**, 675 (2005); I. A. Shovkovy, *Found. Phys.* **35**, 1309 (2005).

[2] M. Huang and I. A. Shovkovy, *Phys. Rev. D* **70**, 051501(R) (2004); *Phys. Rev. D* **70**, 094030 (2004).

[3] R. Casalbuoni, R. Gatto, M. Mannarelli, G. Nardulli, and M. Ruggieri, *Phys. Lett. B* **605**, 362 (2005); **615**, 297(E) (2005).

[4] M. Alford and Q. H. Wang, *J. Phys. G* **31**, 719 (2005).

[5] K. Fukushima, *Phys. Rev. D* **72**, 074002 (2005).

[6] I. Giannakis and H. C. Ren, *Phys. Lett. B* **611**, 137 (2005); *Nucl. Phys.* **B723**, 255 (2005); I. Giannakis, D. f. Hou, and H. C. Ren, *Phys. Lett. B* **631**, 16 (2005).

[7] M. Huang, *Phys. Rev. D* **73**, 045007 (2006).

[8] D. K. Hong, [hep-ph/0506097](#).

[9] E. V. Gorbar, M. Hashimoto, and V. A. Miransky, *Phys. Lett. B* **632**, 305 (2006).

[10] E. V. Gorbar, M. Hashimoto, and V. A. Miransky, *Phys. Rev. Lett.* **96**, 022005 (2006).

[11] K. Iida and K. Fukushima, [hep-ph/0603179](#).

[12] K. Fukushima, *Phys. Rev. D* **73**, 094016 (2006).

[13] E. V. Gorbar, M. Hashimoto, and V. A. Miransky, and I. A. Shovkovy, *Phys. Rev. D* **73**, 111502(R) (2006).

[14] M. Hashimoto, [hep-ph/0605323](#).

[15] O. Kiriyama, D. H. Rischke, and I. A. Shovkovy, [hep-ph/0606030](#).

[16] I. Giannakis, D. Hou, M. Huang, and H. c. Ren, [hep-ph/0606178](#).

[17] M. Buballa and I. A. Shovkovy, *Phys. Rev. D* **72**, 097501 (2005).

[18] I. Shovkovy and M. Huang, *Phys. Lett. B* **564**, 205 (2003); M. Huang and I. Shovkovy, *Nucl. Phys.* **A729**, 835 (2003).

[19] S. B. Rüster, V. Werth, M. Buballa, I. A. Shovkovy, and D. H. Rischke, *Phys. Rev. D* **72**, 034004 (2005); D. Blaschke, S. Fredriksson, H. Grigorian, A. M. Öztaş, and F. Sandin, *Phys. Rev. D* **72**, 065020 (2005); H. Abuki and T. Kunihiro, *Nucl. Phys.* **A768**, 118 (2006).

[20] O. Kiriyama, in preparation.

[21] M. Alford, J. A. Bowers, and K. Rajagopal, *Phys. Rev. D* **63**, 074016 (2001); J. A. Bowers and K. Rajagopal, *Phys. Rev. D* **66**, 065002 (2002).

[22] K. Rajagopal and R. Sharma, [hep-ph/0605316](#).

[23] Lianyi He (private communication).

[24] We have examined the robustness of the relation $T^* \simeq \delta\mu/2$ varying our model parameters and confirmed that it works well as far as $\bar{\mu}$ is not too small.

[25] The upper boundary of this unstable region, $\Delta_0 = 162$ MeV, is lower than that quoted in Refs. [10, 15]. As mentioned earlier, the fact that our parameters do not correspond to the HDL limit yields the difference. To find the unstable window we directly calculated the Meissner mass squared and the resulting critical value of $\Delta/\delta\mu$ is much smaller than the HDL value $\sqrt{2}$.